Ocean Dynamics (2026) 76:19
https://doi.org/10.1007/s10236-026-01776-w

On the contribution of the Gulf stream to high frequency coastal sea level variability

Tal Ezer[1]

Received: 16 October 2025 / Accepted: 13 January 2026

Abstract
Long-term Atlantic Ocean and Gulf Stream (GS) variability were linked in past studies to coastal sea level (CSL) change along the U.S. East Coast – a weakening GS can lead to rise in CSL and increased coastal flooding. However, high frequency variability (HFV) in CSL is, in most cases, attributed to atmospheric weather events. This study is focused on HFV (intraseasonal variations with periods between ~1 week and ~2 months) in the GS and in CSL. First, wavelet and spectral analysis of observations of the Florida Current transport and CSL characterized the HFV in the data, and then idealized numerical simulations were conducted to study the response of CSL to imposed GS variations with known frequencies. Three experiments were conducted: a control run with constant surface and boundary forcing, and two experiments with imposed oscillations in the Florida Current transport into the model domain- a "high-frequency experiment" (HFE) and a "low-frequency experiment" (LFE), where the period of the GS oscillations were ~1–2 weeks and ~1–2 months, respectively. The observations and the model show statistically significant anticorrelation between the GS flow and the CSL, but the LFE resulted in higher GS-CSL correlations and was more like the observations than the HFE was. The results also show large spatial differences in the CSL response to GS variations - the South-Atlantic Bight (SAB) responded more strongly to the LFE while the Mid-Atlantic Bight (MAB) responded more strongly to the HFE. Power spectra of the model simulations show that even small, imposed GS oscillations at high frequency, can interact with natural variability to excite unpredictable CSL variabilities over a wide range of frequencies, including oscillations at much longer time scales than the forcing. The variability in the Florida Current flow generated a northward propagating signal along the GS path and a southward propagating sea level signal along the coast. However, the topography near Cape Hatteras seems to partly block communication between the MAB and the SAB. The study demonstrates the important contribution of high frequency GS variability to CSL variability - better understanding of the role of remote forcing on coastal sea level can help to improve prediction of coastal sea level variations and associated flooding.

Keywords Gulf stream · Florida current · Coastal sea level · Ocean variability

1 Introduction

Links between large-scale Atlantic Ocean variability and coastal sea level (CSL) along the U.S. East Coast have been suggested long time ago from early observations (Montgomery 1938; Blaha 1984; Maul et al. 1985) and early models (Sturges and Hong 2001; Ezer 2001). Numerous studies suggested different ways in which changes over the Atlantic Ocean can affect the coast, for example, through variations in the Gulf Stream (GS), variations in the Atlantic Meridional Overturning Circulation (AMOC), variations in the North Atlantic Oscillation (NAO), or due to other ocean dynamic factors (Leverman et al. 2005; Sallenger et al. 2012; Ezer et al. 2013, 2015, 2025a, 2025b; Gawarkiewicz et al. 2012; Chen et al. 2014; Rhmstorf et al. 2015; Piecuch et al. 2016, 2023; Little et al. 2019; Dangendorf et al. 2021, 2023; Volkov et al. 2019, 2023; Ezer and Dangendorf 2020; Ezer and Updyke 2024). The way that offshore ocean dynamics can affect CSL variability often involves sea level signals that propagate toward the coast by mechanisms

Responsible Editor: Huijie Xue

✉ Tal Ezer
tezer@odu.edu

[1] Center for Coastal Physical Oceanography, Old Dominion University, 4111 Monarch Way, Norfolk, VA 23508, USA

Published online: 14 February 2026

such as barotropic and baroclinic Rossby waves, while coastal-trapped waves (CTW) spread signals along the coast (Huthnance 2004; Hughes and Meredith 2006). The clearer connector between offshore dynamics and CSL is the GS. The GS flows from the Florida Straits (where it is referred to as the Florida Current, FC) along the coast of the South Atlantic Bight (SAB), then it separates from the coast near Cape Hatteras, North Carolina, and turned toward the northeast, offshore of the Mid-Atlantic Bight (MAB); see Fig. 1. Since the GS flow speed is proportional to the sea level slope across the stream (due to the geostrophic balance), variations in the position and/or strength of the GS were found in many studies to be linked with CSL (i.e., weakening GS is correlated with increased sea level near the coast and decreased sea level offshore east of the stream; see for example the study on the Gulf Stream's induced sea level in Ezer et al. 2013). This GS-CSL connection is important for decadal variations, as well as for the potential of climate related AMOC slowdown (Smeed et al. 2014, 2018; Caesar et al. 2018; Dong et al. 2019; Volkov et al. 2023) that may

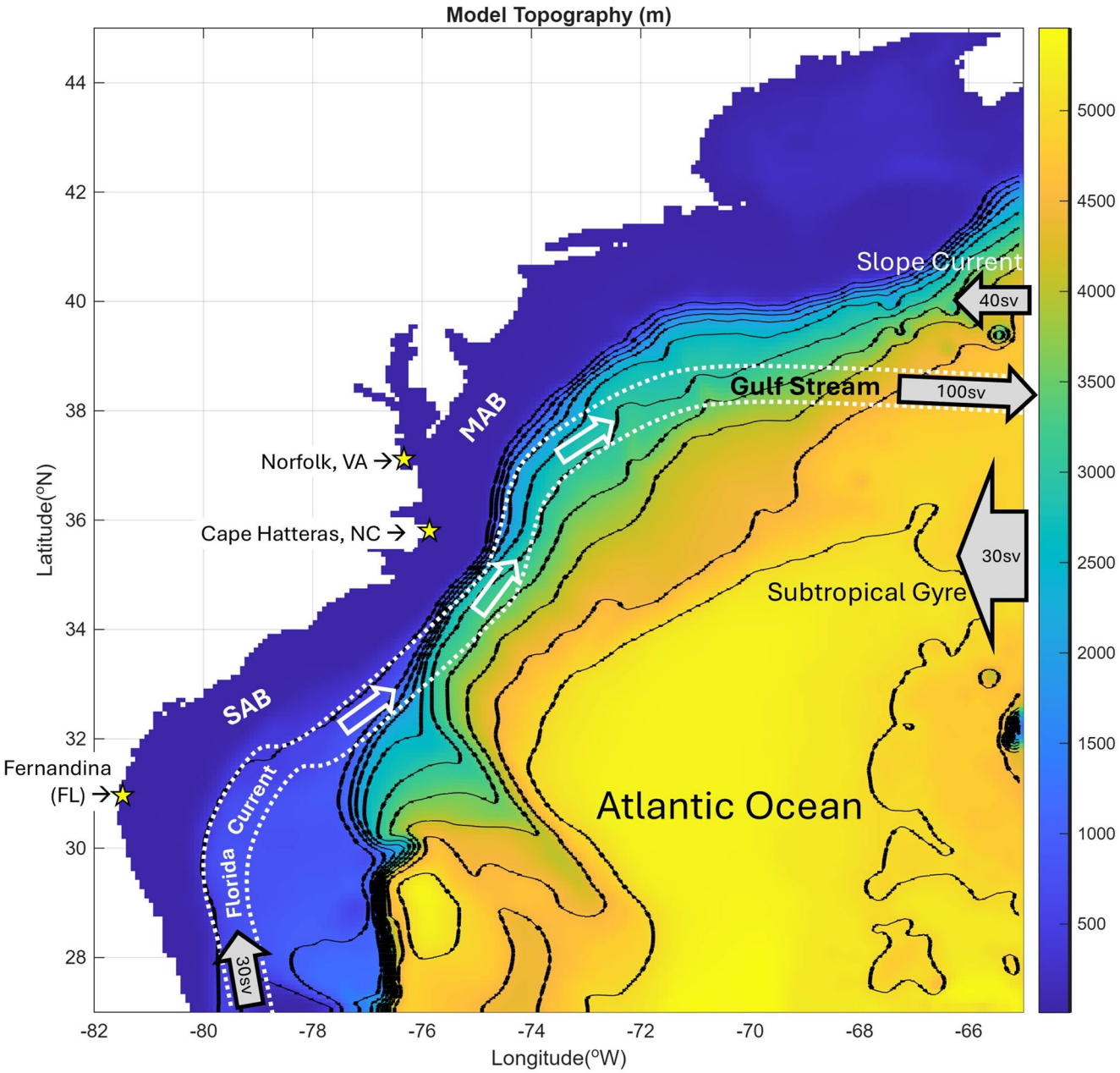

Fig. 1 Bottom topography (depth in meters; color and isobaths) and model domain. Gray wide arrows indicate the location of model imposed mean inflows and outflows with the transport in Sverdrup (1 Sv = 10^6 m^3s^{-1}). Locations of tide gauges in Norfolk and Fernandina are indicated by starts, as well as Cape Hatteras which separates between the Mid-Atlantic Bight (MAB) in the north and the South Atlantic Bight (SAB) in the south

contribute to future sea level rise and increased flooding (Ezer and Atkinson 2014, 2017; Sweet and Park 2014; Goddard et al. 2015; Wdowinski et al. 2016).

Unlike the great interest in remote influence on the coast from long-term variability (time scales of interannual to decadal and longer), less is known about high frequency remote forcing of coastal variability. HFV in coastal dynamics is, in most cases, linked to local drivers such as daily weather events, seasonal wind pattern, river discharges, as well as extreme events like hurricanes, tropical storms and winter storms (Lee and Williams 1988; Kohut et al. 2006; Ezer et al. 2017; Ezer 2018; Park et al. 2022, 2024; Todd et al. 2018). However, some studies show that high frequency variations in the GS can influence coastal sea level (Ezer 2016) and coastal currents (Ezer 2025a) in a similar manner as long-term variabilities do (i.e., weakening GS is linked with rising CSL). Observations and model simulations indeed show significant anticorrelation between HFV in the GS and in CSL (Ezer 2016). The latter study also demonstrates that GS-driven CSL variations are quite different than wind-driven CSL variations in that the coastal response to the GS is more coherent along the entire U.S. coast than the response to wind which is affected by local land and coastal topography. One important topographic feature that influences the CSL-GS relations is Cape Hatteras, which separates between the SAB in the south, where the GS is flowing closer to the coast, and the MAB in the north, where the GS is flowing away from the coast in deep waters. Several studies thus found different sea level response to forcing in the SAB and the MAB (Piecuch et al. 2016; Valle-Levinson et al. 2017; Domingues et al. 2018; Ezer 2019). These differences between the SAB and the MAB will be assessed here by comparing the coastal response in locations north and south of Cape Hatteras.

Since the goal here is to assess the impact on the coast from HFV in the GS, this forcing must be isolated from other forcing- in particular, eliminating variations in the wind. To do that, the study follows on the footsteps of Ezer (2016), which used regional ocean circulation model with constant surface forcing (heat and wind), but with time-dependent oscillation in the GS transport (which is applied through the lateral open boundary conditions of the model, see Fig. 1). Unlike Ezer (2016), who conducted short simulations of 60 days, each one with one forced frequency, here, longer simulations of one year were conducted with oscillations of multiple frequencies. The goal was to see if the response at the coast includes only the forced oscillations, or that multiple forced oscillations can produce a spectrum of CSL oscillations like those seen in observations. Since the GS produces natural mesoscale variability from its instability, experiments with and without forced oscillations can tell us about the interaction of forced oscillations with the natural variability of the GS. These simulations over 360 days are long enough to capture many cycles for conducting spectral analysis. However, one may acknowledge that these idealized simulations cannot last much longer without more realistic surface conditions that include, for example, the seasonal surface heat flux and wind. The model results are also compared with observations of the FC transport (Baringer and Larsen 2001; Meinen et al. 2010) and CSL from tide gauges, to see if the model relations between the GS and CSL resemble the observed relations.

The study is organized as follows: first, the observations are described and analyzed in Sect. 2, then the model setting and the experiments conducted are described in Sect. 3, the results are described in Sect. 4, and finally a summary and conclusions are offered in Sect. 5.

2 Analysis of the Florida current transport and coastal sea level observations

Daily Florida Current (FC) transport from a cable across the Florida Strait (at ~27°N) has been recorded by NOAA/Atlantic Oceanographic and Meteorological Laboratory since the 1980 s (Baringer and Larsen 2001; Meinen et al. 2010; www.aoml.noaa.gov/phod/floridacurrent/). However, there were gaps in the data during 1998–2000 and more recently since 2024, so the focus is on data from 2001 to 2003. Hourly water level records from 2 locations (Fig. 1) were obtained from NOAA tide gauges (https://tidesandcurrents.noaa.gov/), one location in the SAB (Fernandina, Florida; near 31°N) and one in the MAB (Norfolk, Virginia; near 37°N). The latter location was the subject of many sea level studies (Ezer et al. 2013; Ezer 2019, 2020, 2022) because of the impact of sea level rise on flooding in this region, and past studies that link CSL there to variations in the GS. In some cases, daily anomalies were calculated to remove daily wind and tide fluctuations and to allow comparisons with the daily FC data.

Two types of analysis tools are used – a wavelet analysis that can handle non-stationary data and provides coherence between two time series (Grinsted et al. 2004), and a standard spectral analysis to identify specific periods of oscillations. Figures 2 and 3 show the wavelet analyses that compare the FC with the CSL at Fernandina and Norfolk, respectively. Variations in the FC transport (Fig. 2a) indicate significant variability at periods between about 5–30 days, but these peaks change randomly over time. There is also a large energy in a lower frequency band near the semi-annual period (most significant from middle 2022 to early 2023). Variations in CSL at Fernandina (Fig. 2b) show similar chaotic high-frequency energy peaks as in the FC. These high-frequency, non-stationary oscillations show coherency

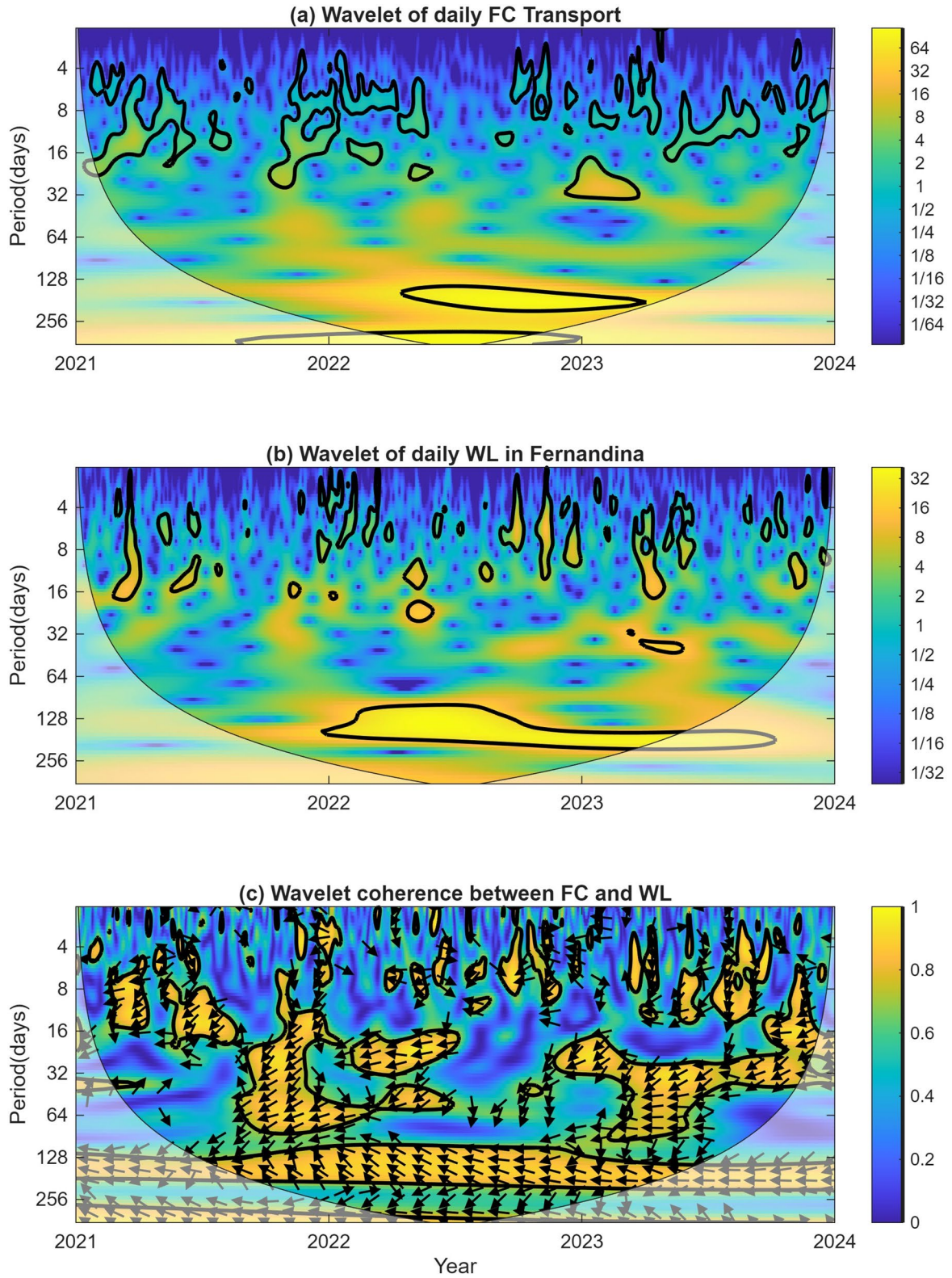

Fig. 2 Wavelet analysis of **a** daily Florida Current (FC) transport observations, **b** daily water level (WL) observations in Fernandina, and **c** coherence between the FC and the WL data. Light black line is the cone of influence where the results are reliable. Yellow color indicates a stronger power in **a** and **b** and a larger coherence in **c**; the most significant regions are indicated by heavy black lines. In **c**, most arrows are pointed left, which indicate negative correlations. Arrows pointed down indicate that the FC is leading the WL by 90°. Linear correlation coefficient between FC and WL over the 3 years is $R=-0.5$ (significant level > 99.9%)

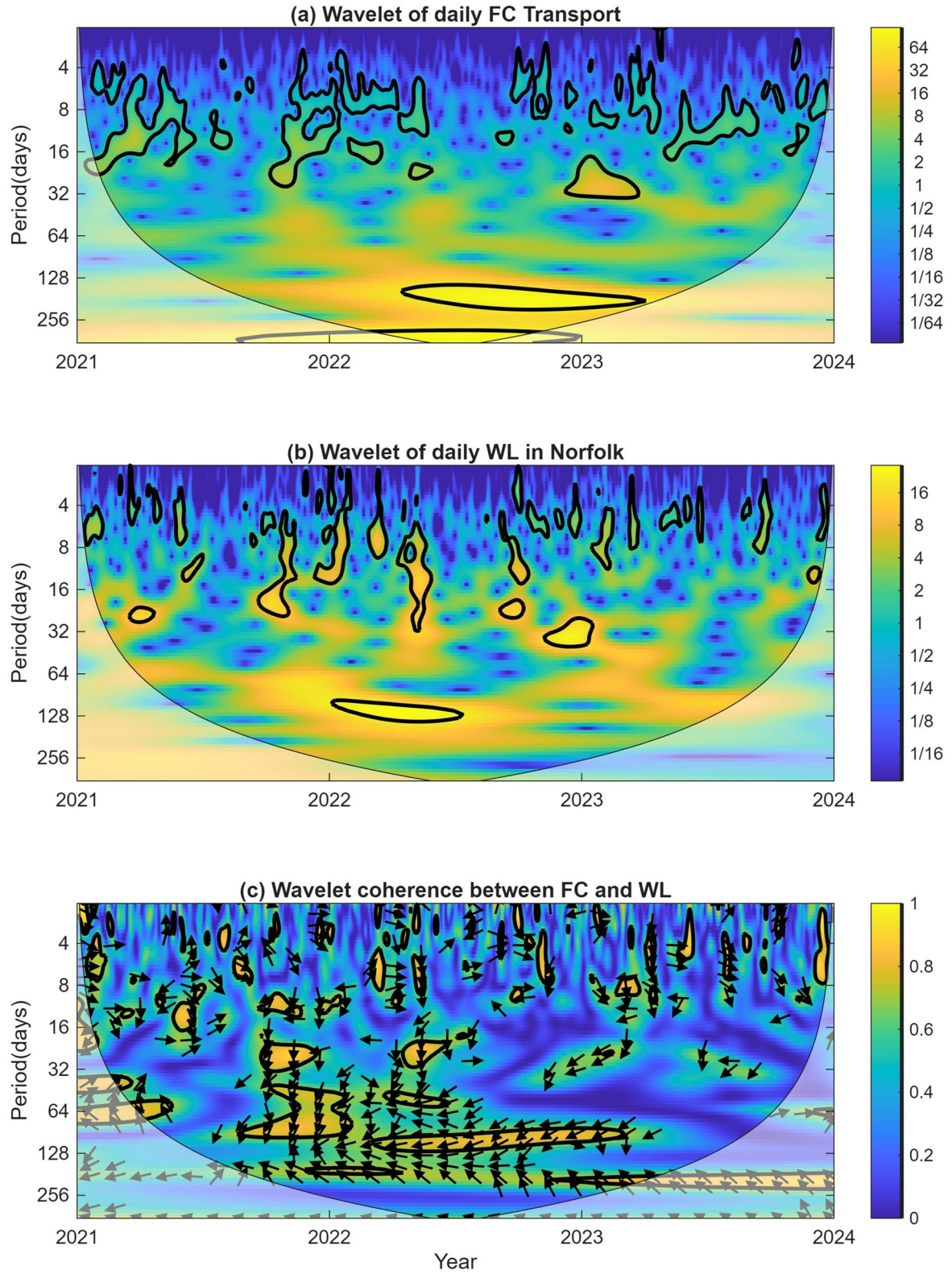

Fig. 3 Same as Fig. 2, but for Norfolk tide gauge. Linear correlation coefficient between FC and WL over the 3 years is R=−0.2 (significant level>99.9%)

between the FC and CSL (Fig. 2c), but larger areas of coherency are also seen in lower frequencies. The pointing of the arrows to the left in Fig. 2c indicates a negative correlation, and indeed, the linear correlation coefficient between the two records is R=−0.5 (with statistical confidence over 99.9%). The wavelet analysis and coherence of the FC with the sea level in Norfolk (Fig. 3) is qualitatively quite like that in Fig. 2, but with smaller regions of significant coherency, especially for periods longer than a month. Therefore, the correlation coefficient of sea level in Norfolk with the FC is lower, R=−0.2 (but it is still statistically significant at the 99.9% level). The fact that sea level in Fernandina (in the SAB) has more significant energy at low frequencies while sea level in Norfolk (in the MAB) has more significant energy as higher frequencies, was later explained by the model experiments.

The wavelet analysis indicates a non-stationary high-frequency variability that changes from month to month and from year to year, so next a spectral analysis is conducted for each year, to find the periods of variability involved in each year. Examples of the Florida Current variations and the power spectrum for each year between 2021 and 2023 are shown in Fig. 4. There are great differences between the three years with no clear seasonal cycle that is evident in all years. The focus here will be on the existence of intra-seasonal high-frequency oscillations with periods ranging from ~1 week to ~2 months. The most energetic peaks change from year to year, they are: 15, 22, 36 and 61 days in 2021, 26, 46 and 73 days in 2022, and 28, 33, 47 and 73 days in 2023. The source of these oscillations can be local wind variations and mesoscale dynamics (Lee and Williams 1988; Meinen et al. 2010; Frajka-Williams et al. 2013). The goal of this study is to assess if these HFV in the FC can contribute to the variability of CSL. The CSL of the two locations (Figs. 5 and 6) show considerable HFV ranging from ~1 week to ~2 months, but not necessarily at the same periods as in the FC (Fig. 4); correlations between the GS and CSL will be discussed later. The variability shows significant differences between the two sites and from year to year. For example, during 2021 and 2022 sea level in Norfolk had more energetic HFV than Fernandina did, but not in 2023. Some periods tend to repeat in multiple years at the two locations, such as 14–15 days, 23–24 days, 33 days, and 52 days. Also, in 2022 both locations had a peak more energetic than the HFV with a period of 122 days (not completely shown). A common oscillation with the same period at the two locations suggests that a large-scale change beyond the coast can affect the entire region, such as variations in AMOC or NAO. For example, between April to July 2022 there is an unusual increase in the FC transport (Fig. 4c) accompanied by a decreased sea level in both Fernandina (Fig. 5c) and Norfolk (Fig. 6c); during the same period the NAO index shifts from negative to positive (not shown). This is consistent with studies that show that sea level rises along the U.S. east coast during periods of low NAO index (Ezer 2015; Goddard et al. 2015).

To evaluate more quantitatively the relations between the GS (as measured by the FC transport) and CSL (as measured by tide gauges), linear correlation coefficients between the two are calculated from daily values and shown in Fig. 7a for each year (another year, 2020, was added to the previous analysis to better show trends). While the correlations indicate that less than 30% of the total CSL variability is directly linked to the GS (maximum R^2~0.3), the correlations are statistically significant at over the 95% level (P<0.05) for all cases except at Norfolk in 2020. In Fernandina, the significance level of the correlation is as high as 99.99%. Correlations are higher in the SAB (Fernandina) near the FC than they are farther north in the MAB (Norfolk), and this is also confirmed by the larger wavelet coherence in Fernandina vs. Norfolk (Figs. 2c and 3c). An interesting result is that correlations increase with decreasing in mean FC transports from 2020 to 2023. Figure 7b shows that when the variability of the FC increases (as in 2022), the CSL variability increases as well, further supporting the hypothesis that the two are connected. However, statistical correlation does not necessarily mean causation, for example, storm events passing the U.S. east coast can affect both the GS and CSL. To assess if variations in the GS are in fact causing variations in CSL, controlled experiments with a numerical ocean circulation model will be used (see next section).

3 Model experiments

An idealized numerical ocean circulation model is used to assess the potential impact of HFV in the GS on CSL. The model grid, forcing, and boundary conditions are identical to the model used in Ezer (2016). The basic code is based on the generalized coordinate ocean circulation model with a terrain-following vertical grid (Mellor et al. 2002; Ezer and Mellor 2004). The model has 21 layers with higher resolution near the surface and a cartesian horizontal grid with 1/12° resolution (~6–8-km grid size). The model is driven at the surface by a constant mean wind (see Ezer 2016) and zero surface heat and freshwater fluxes. The presented results are simulations after several months of adjustment starting from observed mean initial condition (see Ezer 2016 for details). Since the simulations are meant to capture HFV cycles, they are conducted over a relatively short period (1 year), which allows a frequent output at intervals of 3 hours (in comparison, simulations in Ezer 2016 lasted only 60 days). The simulations are long enough to capture many HFV cycles, but short enough to ignore realistic forcing such as seasonal

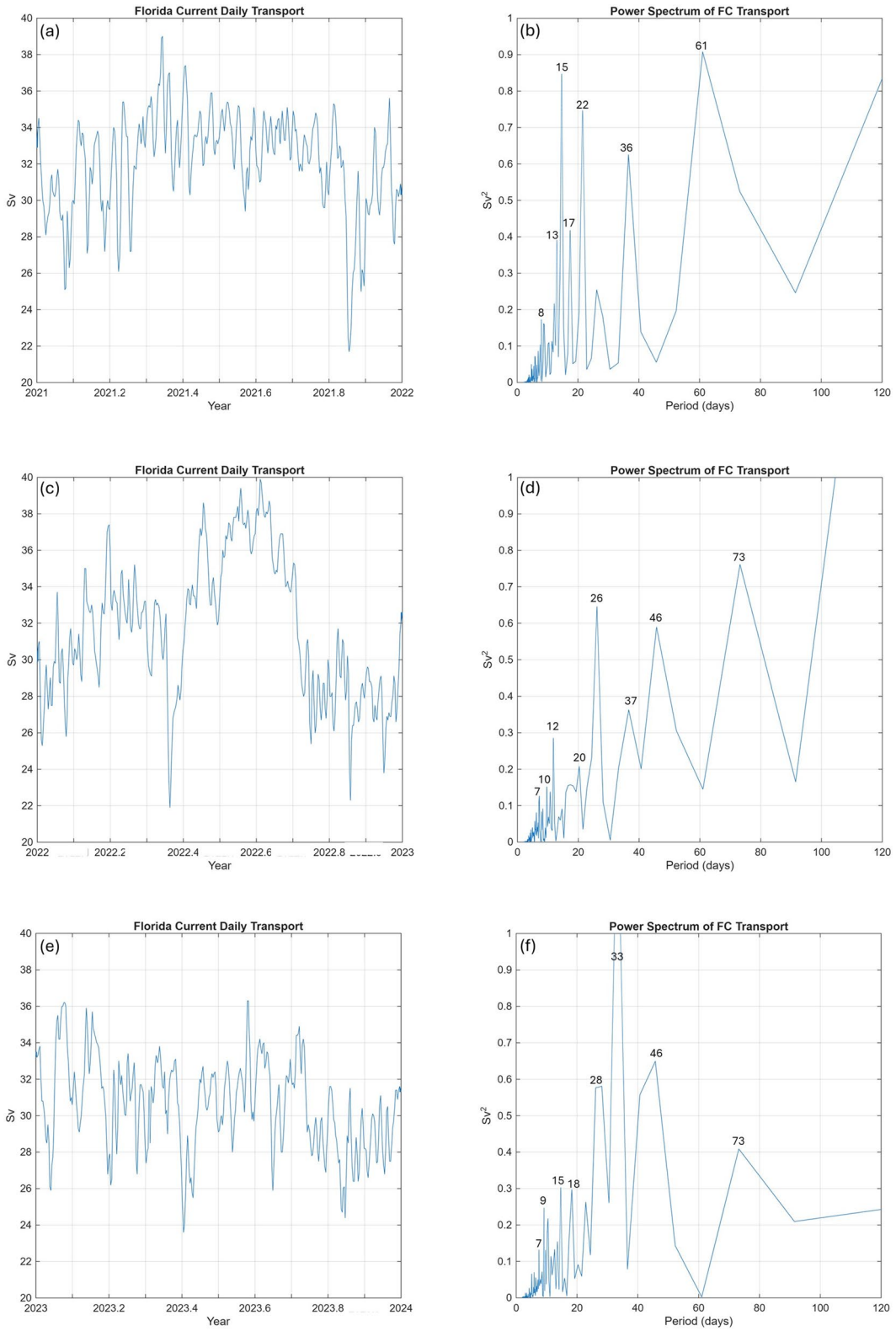

Fig. 4 Time series (left panels) of daily observations of the Florida Current and the power spectrum (right panels) of each year (2021–2023; from top to bottom). The periods (in days) of major peaks are indicated

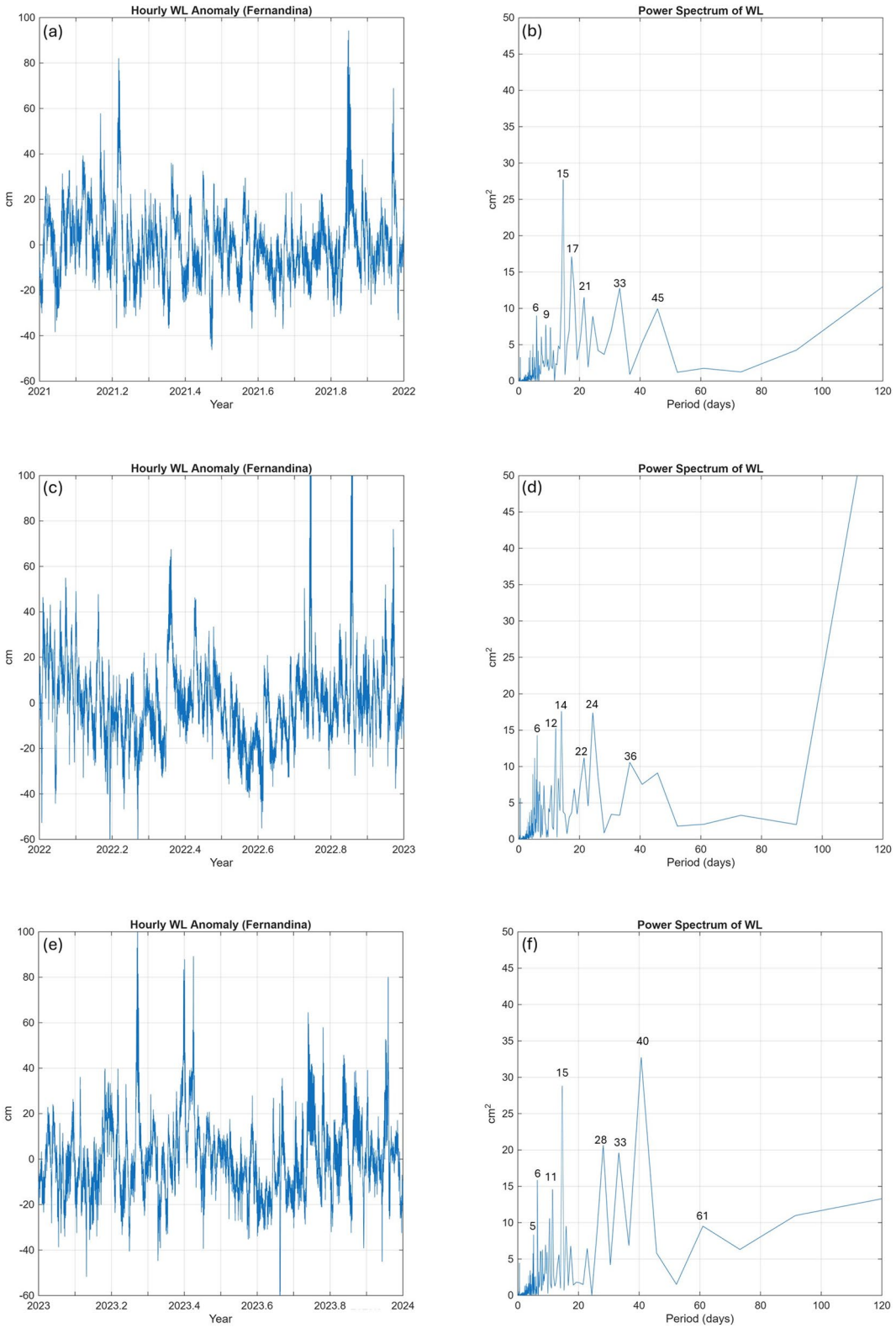

Fig. 5 Same as Fig. 4, but for hourly water level anomaly in Fernandina, FL (~31°N; see Fig. 1)

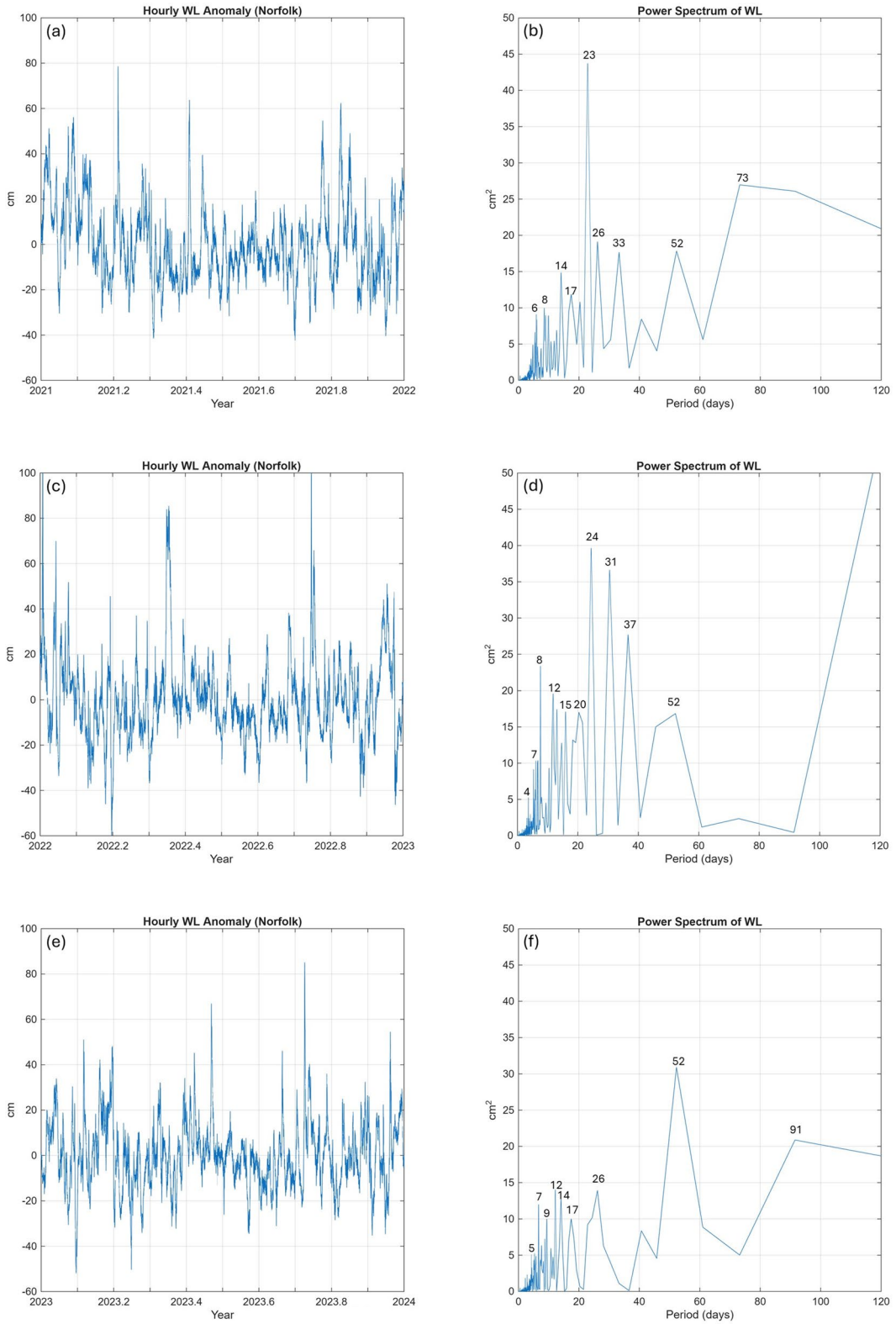

Fig. 6 Same as Fig. 5, but for hourly water level anomaly in Norfolk, VA (~37°N; see Fig. 1)

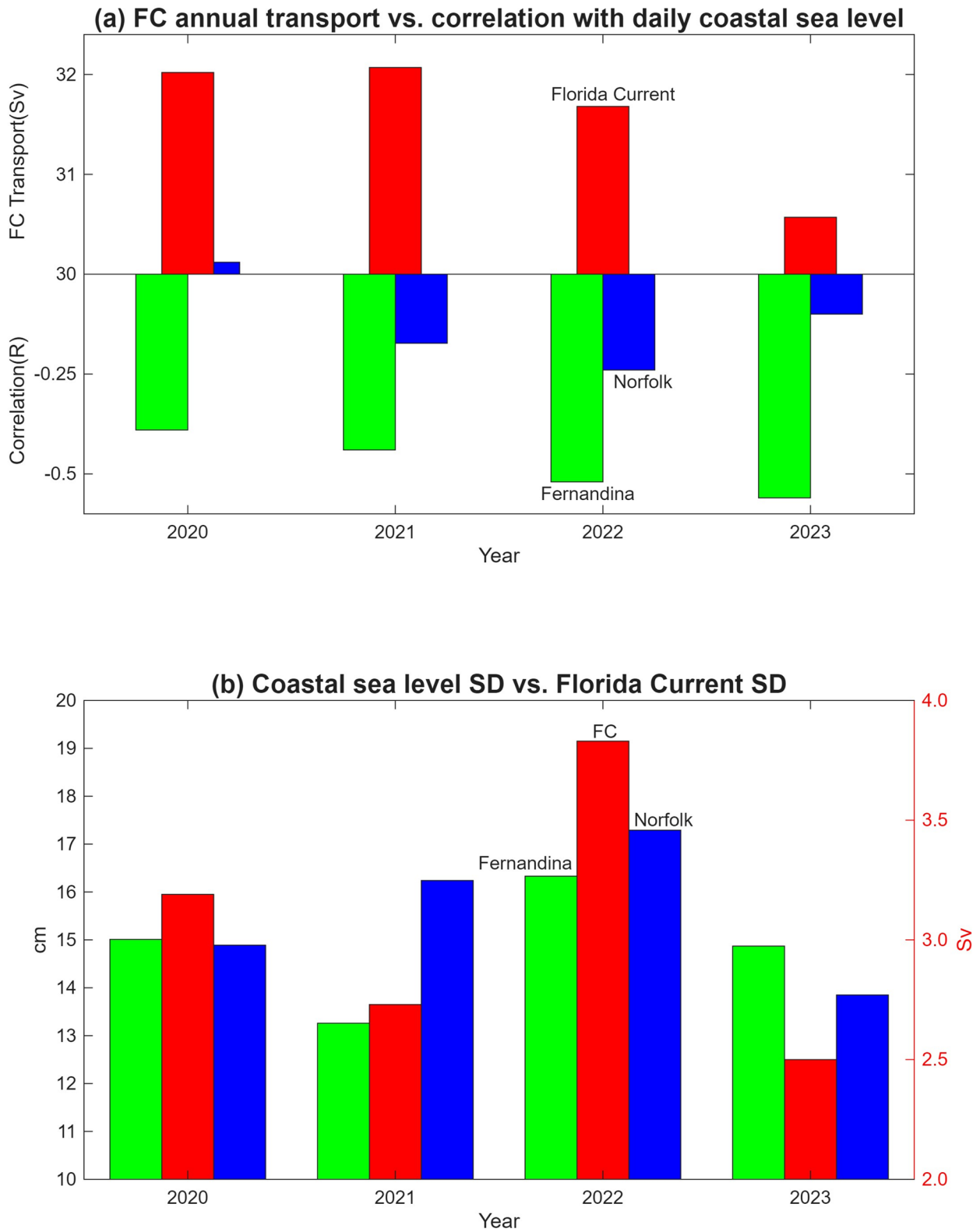

Fig. 7 **a** Annual mean transport of Florida Current (FC, red bars) and correlation coefficient between the daily transport and water level in Fernandina (green bars) and Norfolk (blue bars). Correlations with |R|>0.1 have significant level over 95% ($P<0.05$), so that all cases except Norfolk in 2020 are statistically significant. **b** Standard Deviation (SD) of the FC transport (red bars; right y-axis) and water levels (green and blue bars; left y-axis)

heat flux and wind variability. The idea is to isolate the GS-induced variability by having lateral boundary conditions as the only time-dependent forcing without variations in surface forcing. Inflow and outflow transports are imposed on the eastern and southern open boundaries (Fig. 1) where vertically mean transports are imposed; velocities at each level are dynamically adjusted by the model due to the density field near the boundary within a buffer zone of ~1°. The inflow transports include the Florida Current (FC) in the south, and the Slope Current and the Subtropical Gyre inflows in the east - they are balanced by 100 Sv (1 Sv = 10^6 m^3/s) outflow transport of the Gulf Stream. Three experiments were conducted, starting from the same initial conditions and lasting for a year each:

Experiment #1: a control run with fixed inflows and outflows as described above, so the only variability is the natural mesoscale variability due to the GS meandering instability.
Experiment #2: High-Frequency Experiment (HFE) with oscillations of ±5 Sv at periods of 7 days and 12 days imposed on the FC inflow (and the GS outflow to conserve the volume).
Experiment #3: Low-Frequency Experiment (LFE), same as experiment #2, but with oscillations at periods of 33 days and 46 days.

The choice of forcing frequencies is based on the typical periods of oscillations seen in the wavelet and spectral analyses. Only a few periods are chosen to make it easier to separate between forced oscillations and other variabilities generated by the dynamics. Figure 8 shows the imposed FC transport and the power spectra in the HFE and LFE cases. The imposed oscillations ignoring low-frequency variabilities with periods longer than about 1.5 months in order to assess what frequencies of CSL variability are generated when the GS includes only distinct known cycles.

4 Results

Figure 9 shows the mean model surface elevation in HFE (which is almost identical to the other experiments, so not all are shown) and the variability (Standard Deviation, SD, which is the Root Mean Square, RMS, of the surface elevation anomaly) of the three experiments. The area of the largest variability is in the GS extension after it has separated from the coast with variability associated with the mesoscale variability of the meandering stream, eddies, and recirculation gyres (Andres et al. 2020). The maximin variability of ~25–30 cm is only slightly less than the observed variability from altimeter data and ocean models of similar resolution which is around 30–40 cm (Chassignet and Xu 2017). The extent of the high variability area here is somewhat smaller than observations, but this is expected since surface wind and heat fluxes as well as interannual variations are neglected in the idealized model. All three experiments have similar maximum variability but very different spatial patterns, showing that the variability away from the coast is mostly driven by internal variability of the GS, and not directly influenced by the imposed HFV in the FC. In the HFE case (Fig. 9d) there is increased variability farther downstream the GS near the MAB – later analysis will further show that indeed, the HFE has a larger impact on the coastal MAB than on the SAB.

Figure 10 shows the correlation between the model surface velocity of the FC near 27°N and sea level over the model domain. In both experiments HFE (Fig. 10a) and LFE (Fig. 10b) the entire coast from Florida to Canada has negative correlations (blue). Positive correlations (red) are found only in locations east of the GS. This result is consistent with past studies that indicate CSL rise when the GS is weakening. While the pattern of correlations is similar in both cases, the LFE case shows larger absolute correlations (both positive and negative) than the HFE, indicating a large coastal response to GS oscillations with periods of about 1–1.5.5 months.

To look closely at the type of variations induced by the GS, Fig. 11 shows the time series of CSL at two locations, one in the SAB around 31°N and one in the MAB around 38°N. Because of the coherent correlations across the SAB and MAB (Fig. 10), choosing slightly different locations did not make any significant difference. Qualitative assessment of the CSL clearly show the opposite change in FC velocity and CSL, for example, in the LFE case (Fig. 11b) when the FC was very weak around day 30 CSL in SAB was extremely high, and around day 240 when the FC was stronger, CSL in SAB was lower. However, there are clearly some CSL variations that are unrelated to the GS, like the low CSL from days 140–180. The variations of CSL in the SAB (blue), close to the FC, are much larger than the variations in the MAB (green) farther downstream the GS path, when the GS is also farther away from the coast. Compared to the mostly wind-driven observed CSL variability (Figs. 5 and 6) of ~40 cm (excluding big storm surges), the GS-induced variability is only up to ~20 cm in the SAB and ~5 cm in the MAB.

Power spectra of the CSL in the three experiments are shown in Fig. 12 – they are clearly very different than the GS forcing in the model (Fig. 8). The control experiment with no time-dependent forcing (Fig. 12ef) produces CSL oscillations at periods ranging from about 2 weeks to 1.5 months – these oscillations, while very small in amplitude, represent the natural variability of the GS system due to

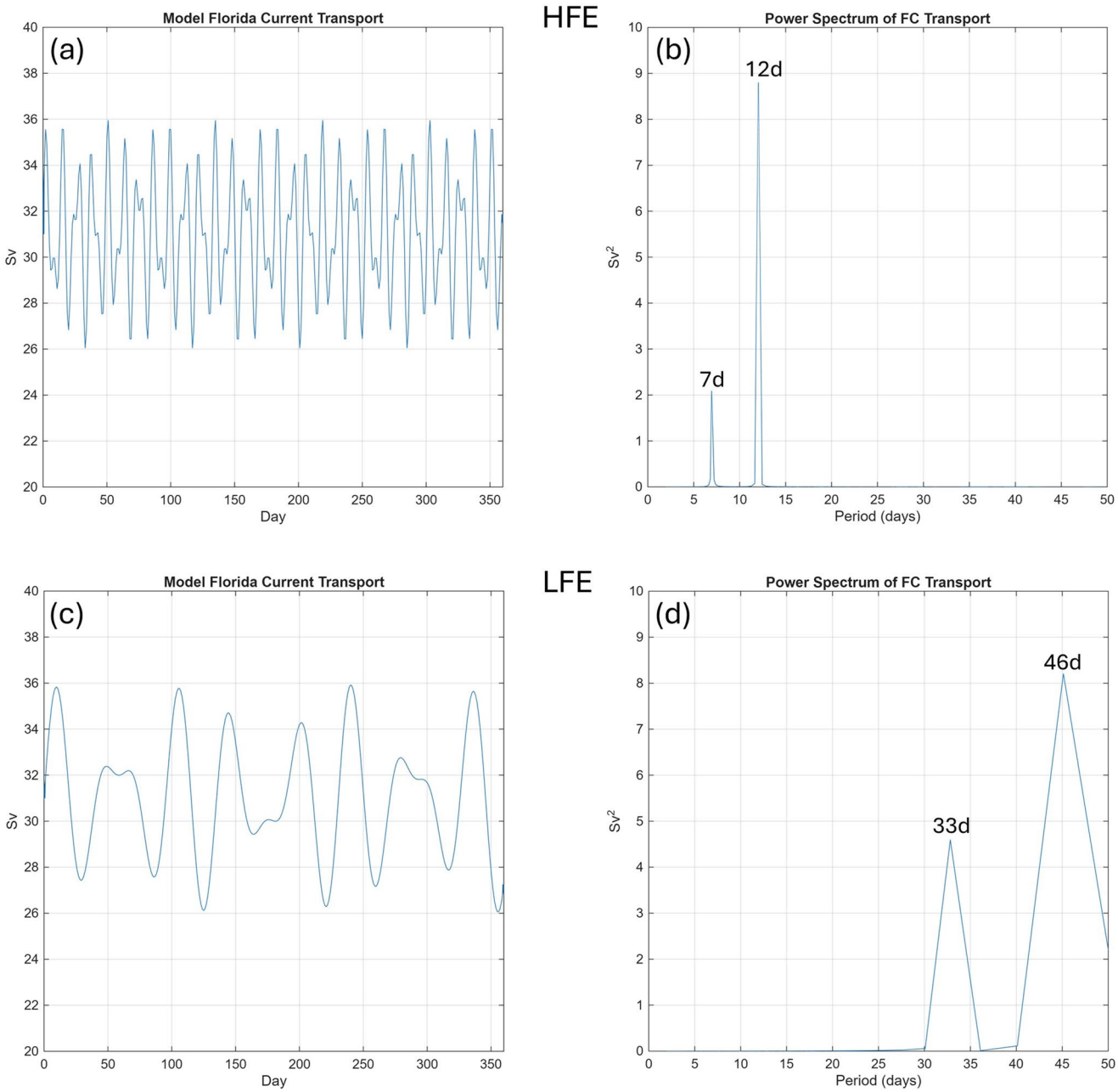

Fig. 8 The imposed model inflow (left) and its spectrum (right) of the Florida Current (see Fig. 1) in the High-Frequency Experiment (HFE; top panels) and the Low-Frequency Experiment (LFE; bottom panels)

instability of the GS, meanders, and mesoscale eddies. The inclusion of even small FC oscillations in HFE and LFE increases the CSL energy by 5–10 times and produces unpredictable frequencies beyond the forcing frequencies; period of peaks ranging from 1 week to 90 days (Fig. 12a-d). There are, however, significant differences between the SAB and MAB (left and right panels of Fig. 12, respectively), and between the HFE and LFE (top and middle panels, respectively). In the MAB, oscillations at periods ~ 33–34 days and ~ 43–45 days appear in all 3 cases, even though only in the LFE case (Fig. 12d) these frequencies were forced on the FC. This indicates some intrinsic modes of the GS system in the MAB. On the one hand, only the CSL in the MAB shows high energy at the 7 and 12 days periods (Fig. 12b) when these frequencies were forced in the HFE case. In the SAB on the other hand, low frequency CSL oscillations dominate, with energetic peaks at periods of 60, 72, and 90 days. While the idealized model results are not intended to reproduce the observations, which are changing from year to year (Figs. 2 and 3), some general characteristics of the

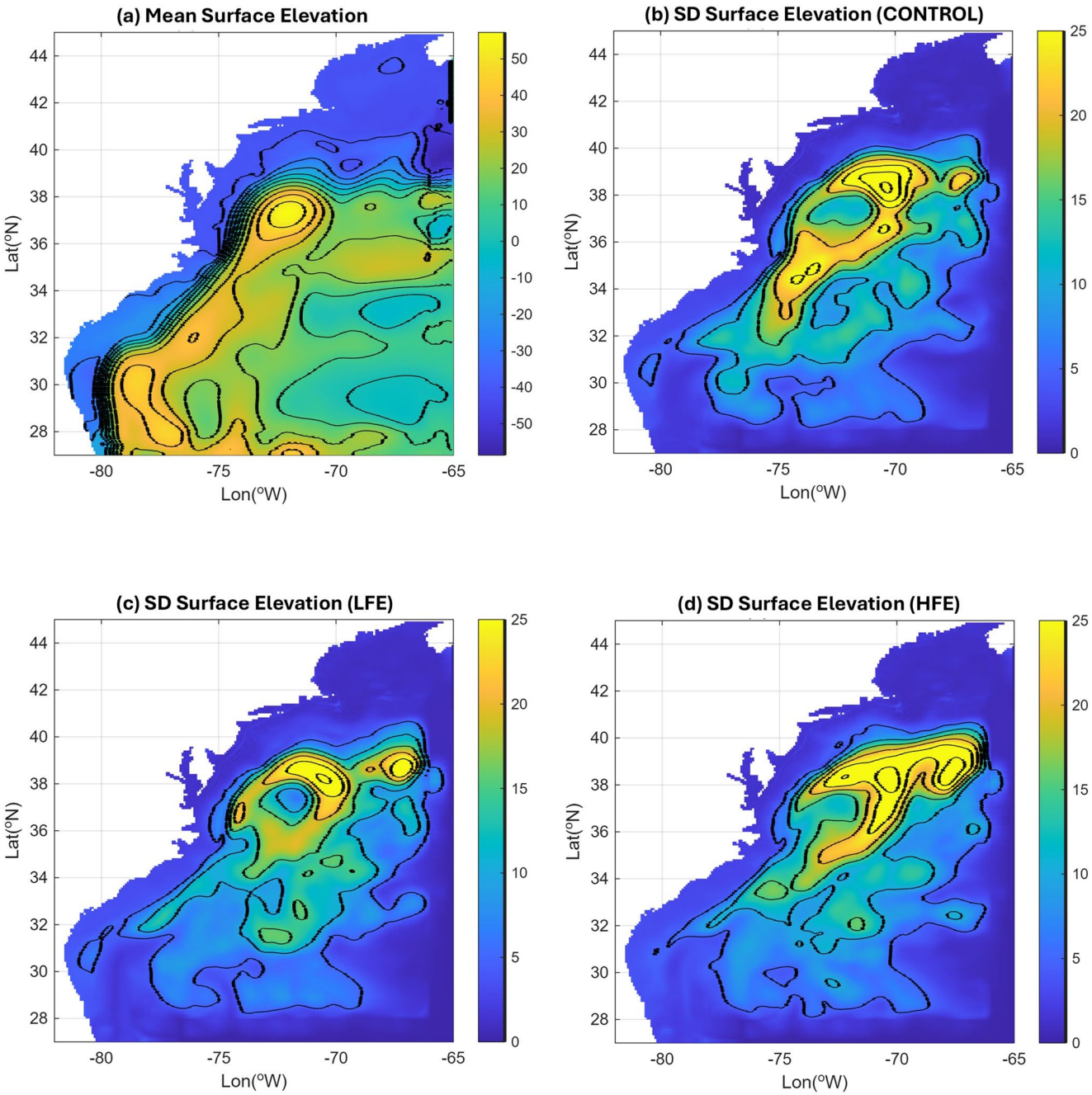

Fig. 9 **a** Annual mean model surface elevation in cm (all 3 experiments are very similar so only the HFE is shown). The standard deviation in the three experiments is shown for **b** the CONTROL, **c** LFE and **d** HFE

CSL variability in the model are consistent with the observations. For example, both the model experiments and the observations show higher energy at high frequencies in the MAB (Norfolk), compared with the SAB (Fernandina). Also, a specific frequency of variability in the FC does not necessarily result in the same frequency in CSL, as the model experiments demonstrate.

Both the idealized model experiments and the observations indicate large differences in the response of CSL in the MAB and in the SAB to offshore variations in the GS. This result is consistent with past studies that show that the coastal areas north and south of Cape Hatters respond differently to remote forcing due to topography and the distance of the GS from the coast (Domingues et al. 2018; Ezer 2016, 2019; Valle-Levinson et al. 2017). The correlation between CSL north and south of Cape Hatteras is shown in Fig. 13a and the correlation between CSL and the GS is shown in Fig. 13b; model correlations (in green) were also compared

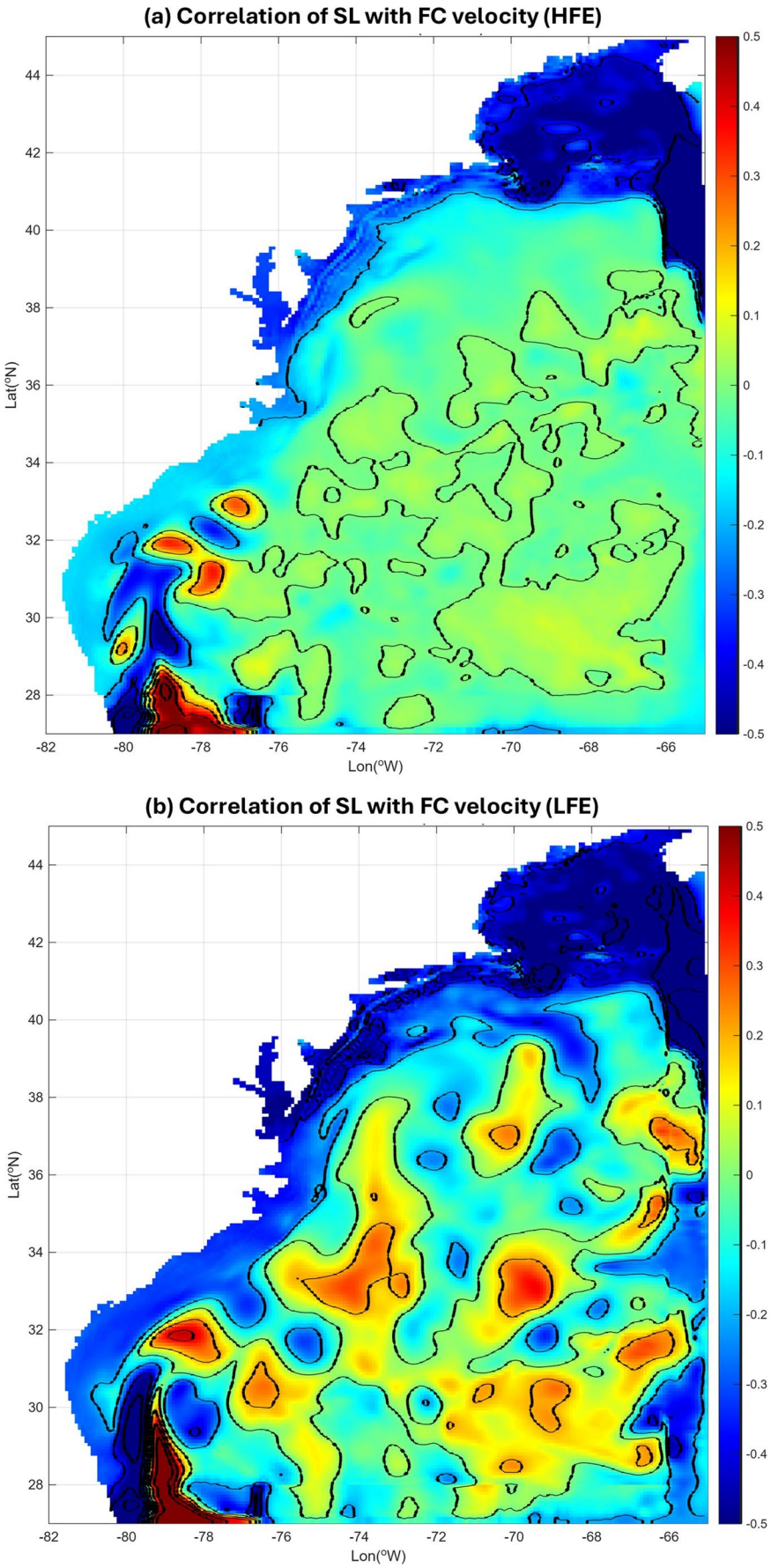

Fig. 10 Correlation coefficient (R) between the surface flow of the GS near the inflow Florida Current (~27°N) and sea level in the model simulations of **a** HFE and **b** LFE. Correlations with |R|>0.05 are significant at 99% ($P<0.01$)

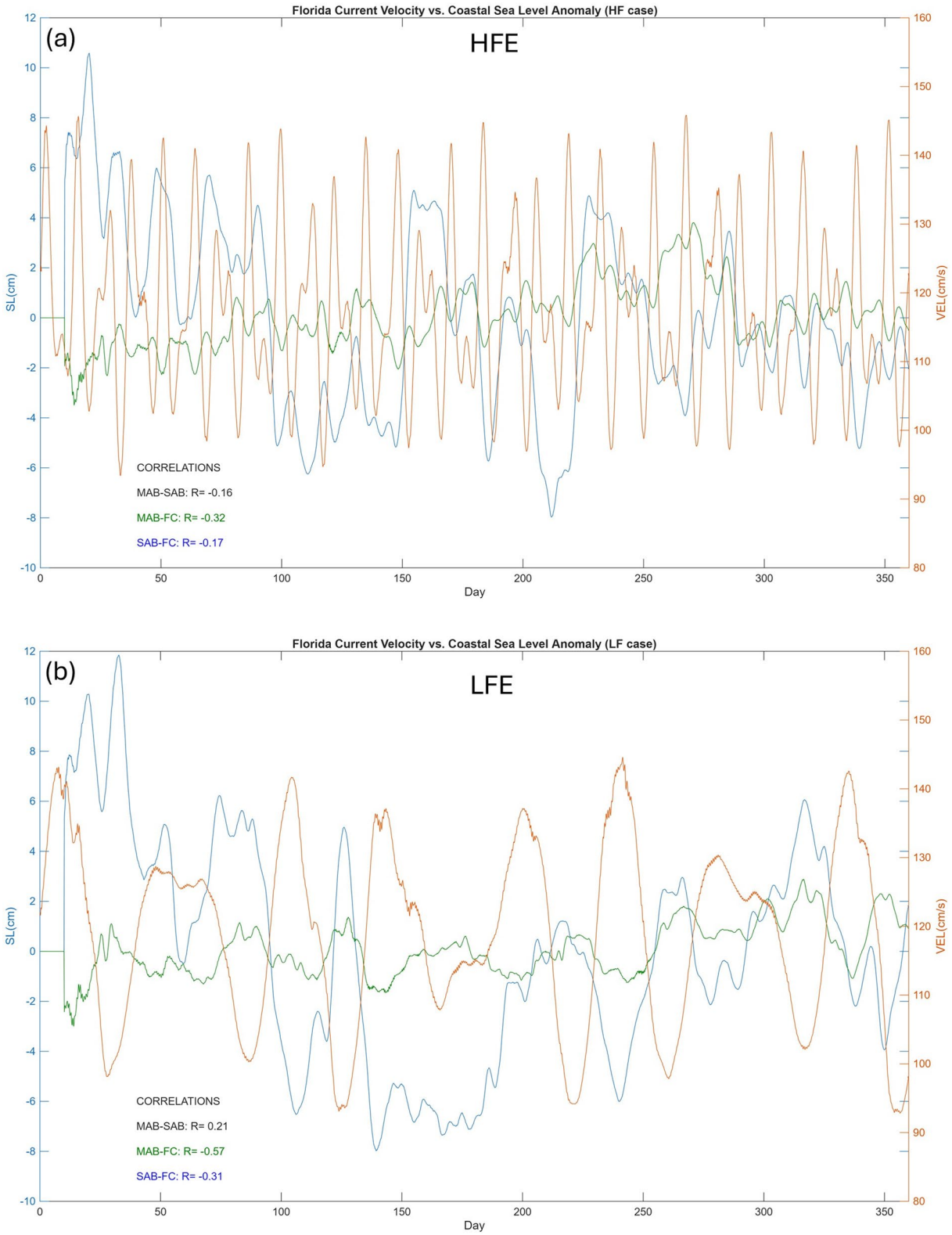

Fig. 11 Florida Current surface velocity in the model (red; in cm/s; right y-axis) and sea level anomaly (in cm; left y-axis) in the MAB (green) and SAB (blue); **a** and **b** are for model experiments HFE and LFE, respectively

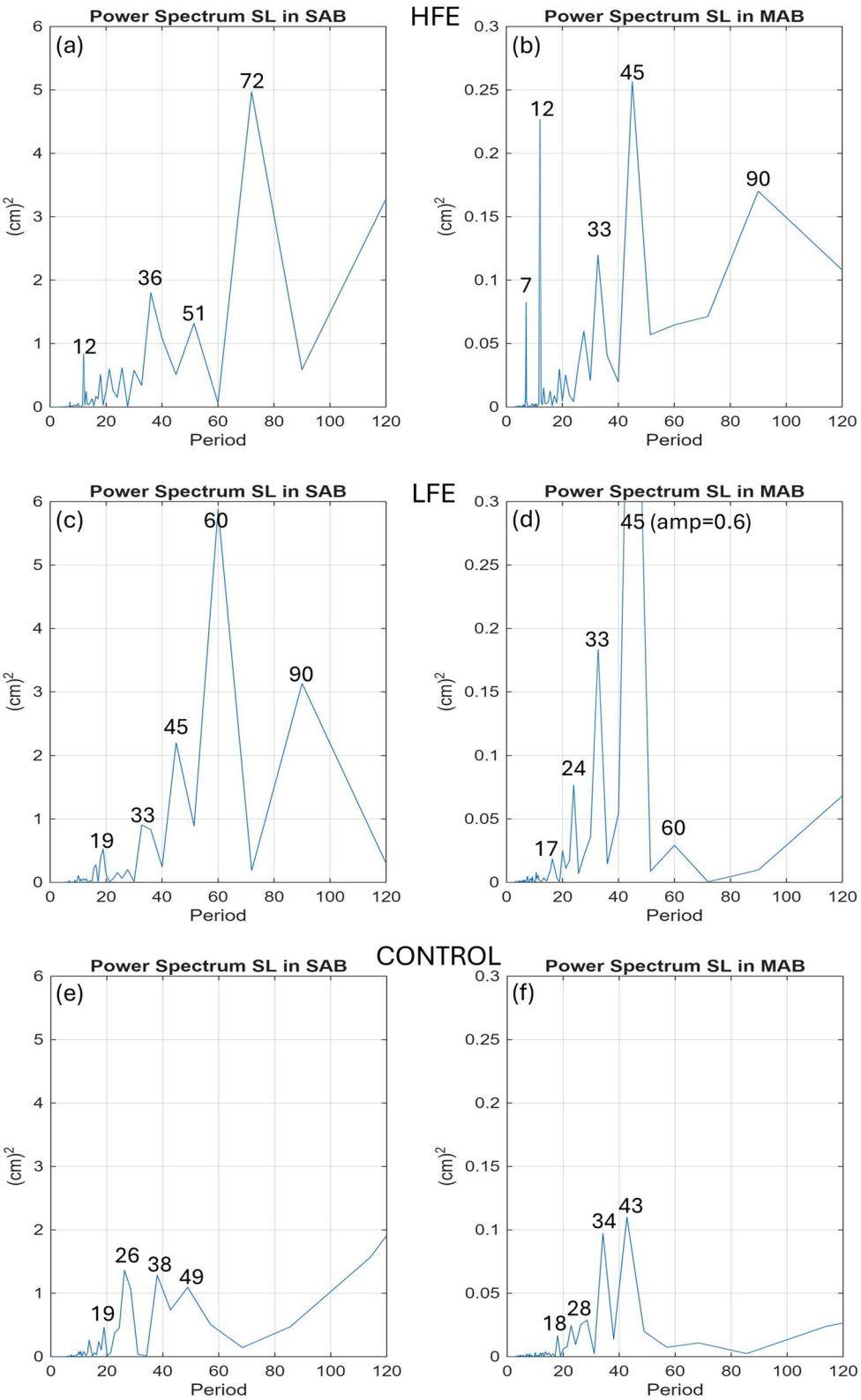

Fig. 12 Power spectra of the three model experiments (top to bottom) for coastal sea level in the SAB (left panels) and MAB (right panels); note the different scales in the left and right panels

with the mean observed correlations (in blue). Surprisingly, the correlations between CSL in the MAB and SAB are completely different in the 3 experiments (Fig. 13a), with negative correlations in the control and HFE, and positive correlations in LFE and the observations. This demonstrates that oscillations with periods around 1–2 months can affect larger extent along the coast, while natural GS variability in the MAB or higher frequency oscillations in the GS have

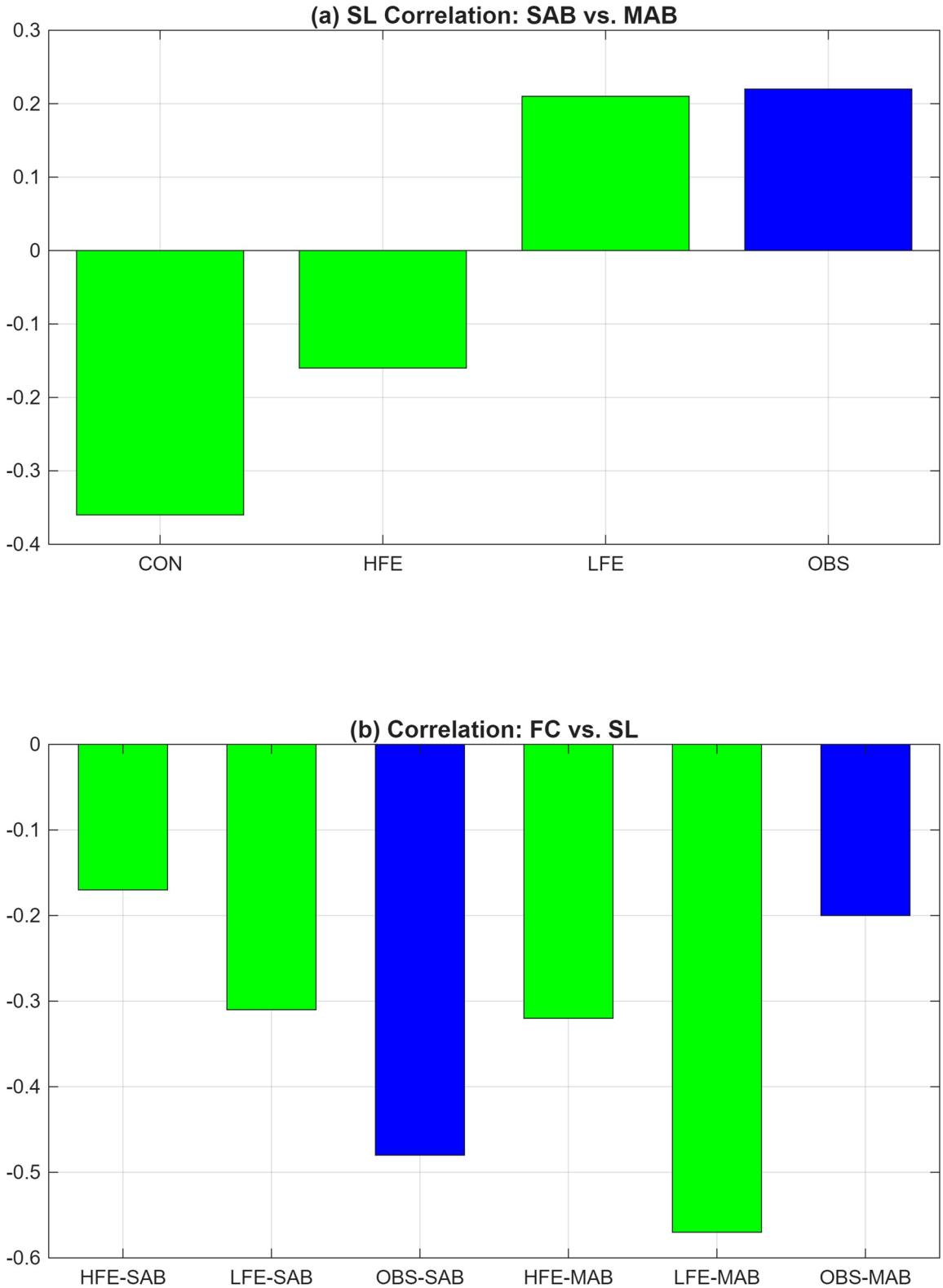

Fig. 13 Comparison of the three model experiments CONTROL, HFE and LFE (green bars) and observations OBS (blue bars). **a** Correlation between sea level in the SAB and sea level in the MAB. **b** Correlations between FC and sea level. The observed values are based on mean of FC transport over 3 years; the model values are based on FC velocity over 1 year for each experiment

difficulty crossing the Cape Hatteras topography separating the MAB from the SAB. The correlation between the GS (i.e., the flow of the FC) and CSL is negative in all the forced model experiments and in the observations with statistically significance of at least 95% (Fig. 13b), indicating that sea level rises when the GS weakens, as expected from theory and past studies. However, the GS may explain only about 3–30% of the total CSL variability (based on R^2) depending on the case and location. Correlations in the LFE case are higher than in the HFE. However, one discrepancy between the model and observations is that in the model correlations are higher in the MAB than in the SAB, while observations show the opposite; this may be due to the neglection of wind variability in the model (Ezer 2016 shows that the response of CSL to variations in the wind is very different than the response to GS variations). In summary, while the model and the observations agree with past studies of the relations between CSL and the GS, the model results demonstrate unexpected sensitivity of CSL to a particular frequency in the GS variability, as well as great spatial variations in the CSL response.

To further investigate the links between variations in the GS and CSL and why the response of sea level in the MAB and SAB are different, Hovmöller diagrams of velocity along the GS path and sea level along the coast are shown in Fig. 14 (LFE case). The impact of topography is clearly seen with different patterns north and south of Cape Hatteras. While the GS flow intensifies near Cape Hatteras, the CSL signal is significantly reduced north of this point. As shown before, periods with a stronger GS flow near the Florida Straits like days 160–220 (Fig. 14b) result in lower CSL in the MAB (Fig. 14a) and vice versa (e.g., days 60 and 350 with weaker flow and higher sea level). The slopes of anomalies show that the velocity signal is propagating northward along the GS path at a speed of ~0.2–0.5 m/s, while the sea level signal along the coast is propagating southward at speeds of ~2–5 m/s. The latter is consistent with coastal barotropic gravity waves that propagate in the northern hemisphere with the coast on the right side and at speeds proportional to square root of depth (the model depth near the coast is just a few meters).

5 Summary and conclusions

The motivation for this study comes from past and recent research that found numerous processes that link coastal processes and sea level variability along the U.S. east coast with remote influence from the Atlantic Ocean. Most of these studies focus on large-scale or long-term open ocean variability including variations in AMOC, the GS, NAO, Rossby Waves, and the subtropical gyre (Leverman et al. 2005; Ezer et al. 2001, 2015, 2013, 2025b; Gawarkiewicz et al. 2012; Chen et al. 2014; Piecuch et al. 2016; Little et al. 2019; Dangendorf et al. 2021, 2023; Volkov et al. 2019, 2023; Ezer and Updyke 2024). Much less is known about how high frequency variability (HFV) in offshore dynamics, such as those associated with the meandering GS, may affect the coast. These HFV are often related to atmospheric variations such as wind and air pressure changes due to daily and seasonal weather, or extreme events such as hurricanes that cause storm surges (Lee and Williams 1988; Kohut et al. 2006; Ezer 2018; Park et al. 2022, 2024). One exception was the study of Ezer (2016), who used a simple GS model to show that high frequency oscillations (periods of 2–10 days) in the GS can produce coherent CSL variations along the coast. The transfer of the offshore signal to the coast involved fast moving barotropic waves and coastal trapped waves that spread the signal along the coast (Huthnance 2004; Hughes and Meredith 2006). However, the experiments in Ezer (2016) involved GS forcing with only one frequency at a time over a short period of only 60 days, thus deeper analyses of the spectrum of frequencies in the observations and the model were not previously possible. The current study follows on the footsteps of the earlier study using the same numerical model but combining several forcing frequencies and conducting longer simulations of 360 days each with high frequency output interval of 3 h (2880 data points for each case). Time series of the daily Florida Current transport and hourly tide gauge sea level data for several years were also analyzed using wavelet and power spectra to assess the high frequency variability that is found in the observations. Another goal was to see if there is a difference in the response of the coast between the SAB when the GS is close to the coast, and the MAB after the GS separated from the coast; this was done by looking at one location north of Cape Hatteras and one location south of Cape Hatters (both in the model and in the observations). Choosing different locations would not make much of a difference in the main results because of the coherence signal found over large coastal areas along the coast.

The main findings are summarized as follows:

1. The observations of the FC and CSL show a wide range of intraseasonal variabilities that dominate the data and conceal less energetic seasonal and interannual variations - this result was previously indicated in the FC measurements of Baringer and Larsen 2001. Peak energy and frequencies change significantly from year to year and from place to place (e.g., between the MAB than the SAB).
2. The observations show larger influence of the GS on CSL during years with a weaker mean GS transport (i.e., from observed FC), or during years with larger GS

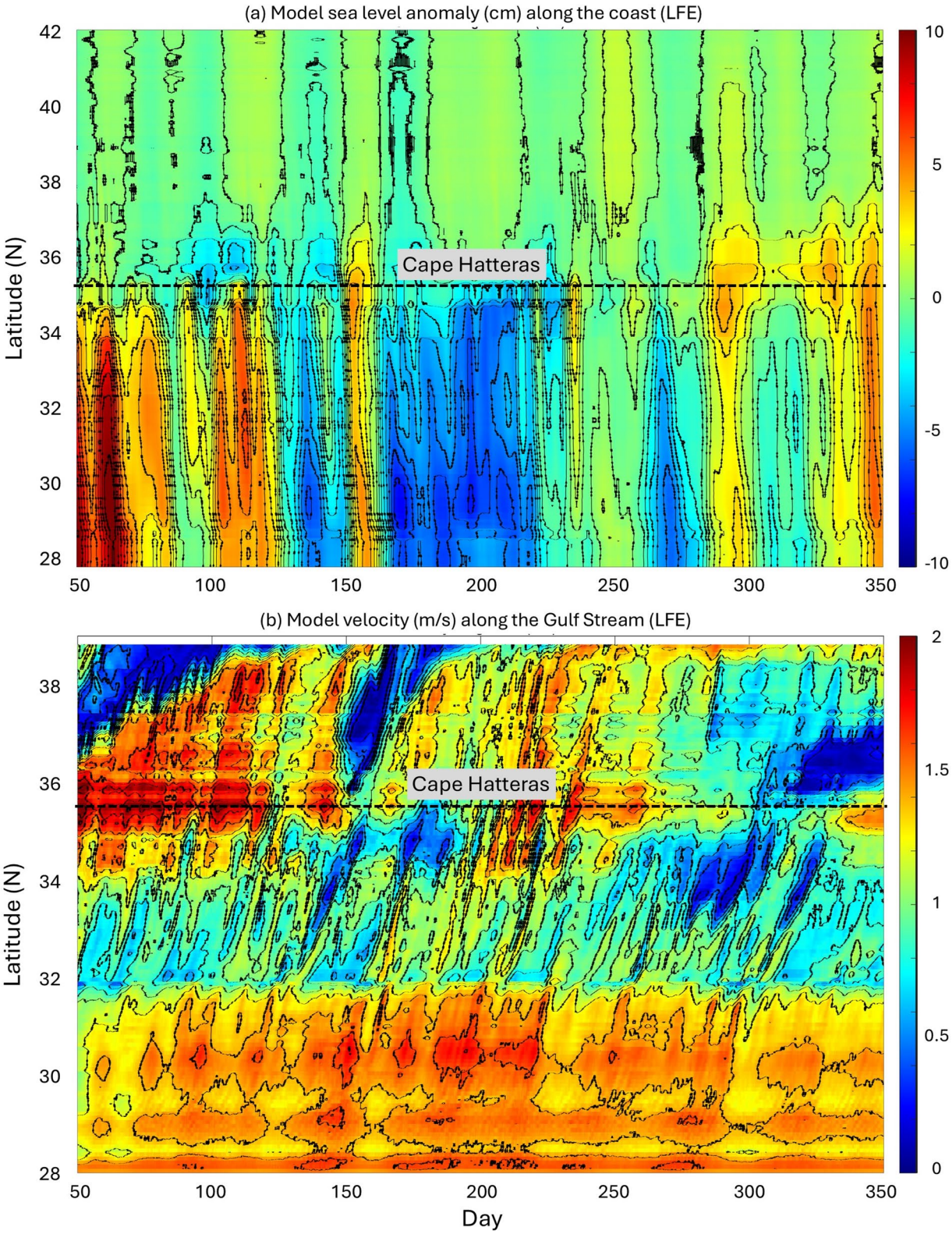

Fig. 14 Hovmöller diagram (value as a function of time and location) of **a** model (LFE case) sea level anomaly along the coast and **b** model velocity along the main path of the Gulf Stream (b only shows the area before the GS turns east). The approximated latitude at Cape Hatteras that separates between the MAB and the SAB is shown by a dashed line

variability. While it is likely that both the GS and the CSL are affected by the same events (like storms), the negative GS-CSL correlation indicates that the two are directly connected, as suggested by dynamic theory and shown in past studies and here.

3. The model shows coherent and statistically significant negative correlation between the surface flow of the GS near the Florida Straits and CSL along the entire U.S. east coast. However, larger correlations (both negative near the coast and positive offshore) are found in the LFE case (FC oscillations of 33 and 46 days) than in the HFE case (FC oscillations of 7 and 12 days).
4. Despite the restricted model forcing with only two FC frequencies at a time, the CSL in the model resulted in a somewhat unexpected wide range of frequencies that are different in the SAB and the MAB. Some natural modes of the system persist independent from the forcing, such as peaks with periods ~ 33–34 days and 43–45 days in the MAB (even when the forcing was at 7 days and 12 days periods, or without any time-dependent forcing), while variations with longer periods of ~ 60–90 days are likely excited from the interaction of the higher frequency forced modes with natural mesoscale dynamics. In general, forcing FC variability at periods of ~ 1–1.5.5 months produced CSL results more like the observations. Forcing FC variability at periods of ~ 1–2 weeks produced CSL oscillations at those frequencies mostly in the MAB while the CSL in the SAB is surprisingly in an opposite phase to CSL in the north. Change in topography at Cape Hatteras and the change in the distance of the GS from the coast between the MAB and the SAB can explain the different coastal response north and south of Cape Hatteras.

In summary, the analysis of the observations and the model's simulations demonstrate the important, but complicated, role of high frequency GS oscillations in contributing to CSL variability. This result makes prediction of sea level variability, sea level rise, and unexpected coastal flooding more difficult to predict. It should be acknowledged though, that even though there is a clear link between a weakening GS and rising CSL with correlations that are statistically significant at 95%–99.9% the high frequency GS variability found here is only responsible for ~ 3%−30% of the total CSL variability, and this link can change dramatically from year to year and from place to place (e.g., between the SAB and MAB). In comparison, on decadal time scales Ezer et al. (2013) found correlations between temporal trends in the GS flow and CSL in the MAB as large as R=−0.85 (i.e., GS may be responsible for ~ 72% of the decadal variability; R^2 = 0.72). Another resent study of surface currents in the MAB found that the GS may contribute ~ 10%−30% of the coastal variability (Ezer 2025a). In conclusion, while the high frequency GS variability cannot be neglected, wind variability (including storms) should still be recognized as a major driver of coastal dynamics.

Acknowledgements The author is affiliated with ODU's Center for Coastal Physical Oceanography (CCPO), which provides office and computational support, and the Institute for Coastal Adaptation and Resilience (ICAR). Reviewers are thanks for useful suggestions for analysis that improved the paper.

Author contributions TE conducted all the research and wrote the manuscript.

Funding No funding was provided for this study.

Data availability Access to all data is provided in the Data Availability Statement.

Declarations

Competing interests The authors declare no competing interests.

References

Andres M, Donohue KA, Toole JM (2020) The Gulf Stream's path and time-averaged velocity structure and transport at 68.5°W and 70.3°W. Deep Sea Res Part I Oceanogr Res Pap. https://doi.org/10.1016/j.dsr.2019.103179

Baringer MO, Larsen JC (2001) Sixteen years of Florida Current transport at 27<Superscript>o</Superscript>N. Geophys Res Lett 28(16):3179–3182. https://doi.org/10.1029/2001GL013246

Blaha JP (1984) Fluctuations of monthly sea level as related to the intensity of the Gulf Stream from Key West to Norfolk. J Geophys Res 89(C5):8033–8042. https://doi.org/10.1029/JC089iC05p08033

Caesar L, Rahmstorf S, Robinson A, Feulner G, Saba V (2018) Observed fingerprint of a weakening Atlantic Ocean overturning circulation. Nature 556:191–196. https://doi.org/10.1038/s41586-018-0006-5

Chassignet EP, Xu X (2017) Impact of horizontal resolution (1/12° to 1/50°) on Gulf Stream separation, penetration, and variability. J Phys Oceanogr 47(8):1999–2021. https://doi.org/10.1175/JPO-D-17-0031.1

Chen K, He R, Powell BS, Gawarkiewicz G, Moore AM, Arango HG (2014) Data assimilative modeling investigation of Gulf Stream warm core ring interaction with continental shelf and slope

circulation. J Geophys Res Oceans 119(9):5968–59991. https://doi.org/10.1002/2014JC009898
Dangendorf S, Frederikse T, Chafik L, Klinck J, Ezer T, Hamlington B (2021) Data-driven reconstruction reveals large-scale ocean circulation control on coastal sea level. Nat Clim Change 11:514–520. https://doi.org/10.1038/s41558-021-01046-1
Dangendorf S, Hendricks N, Sun Q, Klinck J, Ezer T, Frederikse T, Calafat F, Wahl T, Tornquist T (2023) Acceleration of U.S. Southeast and Gulf Coast sea-level rise amplified by internal climate variability. Nat Commun 14:1935. https://doi.org/10.1038/s41467-023-37649-9
Domingues R, Goni G, Baringer N, Volkov D (2018) What caused the accelerated sea level changes along the U.S. East Coast during 2010–2015? Geophys Res Lett 45:13,367-13,376. https://doi.org/10.1029/2018GL081183
Dong S, Baringer MO, Goni GJ (2019) Slow down of the Gulf Stream. Sci Rep 9:6672. https://doi.org/10.1038/s41598-019-42820-8
Ezer T (2001) Can long-term variability in the Gulf Stream transport be inferred from sea level? Geophys Res Lett 28(6):1031–1034. https://doi.org/10.1029/2000GL011640
Ezer T (2015) Detecting changes in the transport of the Gulf Stream and the Atlantic overturning circulation from coastal sea level data: the extreme decline in 2009–2010 and estimated variations for 1935–2012. Glob Planet Change 129:23–36. https://doi.org/10.1016/j.gloplacha.2015.03.002
Ezer T (2016) Can the Gulf Stream induce coherent short-term fluctuations in sea level along the U.S. East Coast?: a modeling study. Ocean Dyn 66(2):207–220. https://doi.org/10.1007/s10236-016-0928-0
Ezer T (2018) On the interaction between a hurricane, the Gulf Stream and coastal sea level. Ocean Dyn 68:1259–1272. https://doi.org/10.1007/s10236-018-1193-1
Ezer T (2019) Regional differences in sea level rise between the Mid-Atlantic Bight and the South Atlantic Bight: is the Gulf Stream to blame? Earths Future 7(7):771–783. https://doi.org/10.1029/2019EF001174
Ezer T (2022) A demonstration of a simple methodology of flood prediction for a coastal city under threat of sea level rise: the case of Norfolk, VA, USA. Earths Future. https://doi.org/10.1029/2022EF002786
Ezer T (2025a) Surface currents in the Mid-Atlantic Bight: the role of the Gulf Stream versus wind. Front Mar Sci. https://doi.org/10.3389/fmars.2025.1645286
Ezer T (2025b) The Gulf stream: its history and links to coastal impacts and climate change. Ann Rev Mar Sci Vol 18. https://doi.org/10.1146/annurev-marine-040224-120037
Ezer T, Atkinson LP (2014) Accelerated flooding along the U. S. East Coast: on the impact of sea level rise, tides, storms, the Gulf Stream and the North Atlantic Oscillations. Earths Future 2(8):362–382. https://doi.org/10.1002/2014EF000252
Ezer T, Atkinson LP (2017) On the predictability of high water level along the U.S. East coast: can the Florida current measurement be an indicator for flooding caused by remote forcing? Ocean Dyn 67(6):751–766. https://doi.org/10.1007/s10236-017-1057-0
Ezer T, Dangendorf S (2020) Global sea level reconstruction for 1900–2015 reveals regional variability in ocean dynamics and an unprecedented long weakening in the Gulf Stream flow since the 1990s. Ocean Sci 16(4):997–1016. https://doi.org/10.5194/os-2020-22
Ezer T, Mellor GL (2004) A generalized coordinate ocean model and a comparison of the bottom boundary layer dynamics in terrain-following and in z-level grids. Ocean Model 6(3–4):379–403. https://doi.org/10.1016/S1463-5003(03)00026-X
Ezer T, Updyke T (2024) On the links between sea level and temperature variations in the Chesapeake Bay and the Atlantic meridional overturning circulation (AMOC). Ocean Dyn 74:307–320. https://doi.org/10.1007/s10236-024-01605-y
Ezer T, Atkinson LP, Corlett WB, Blanco JL (2013) Gulf Stream's induced sea level rise and variability along the U.S. mid-Atlantic coast. J Geophys Res Oceans 118:685–697. https://doi.org/10.1002/jgrc.20091
Ezer T, Atkinson LP, Tuleya R (2017) Observations and operational model simulations reveal the impact of hurricane Matthew (2016) on the Gulf Stream and coastal sea level. Dyn Atmos Oceans 80:124–138. https://doi.org/10.1016/j.dynatmoce.2017.10.006
Frajka-Williams E, Johns WE, Meinen CS, Beal LM, Cunningham SA (2013) Eddy impacts on the Florida current. Geophys Res Lett 40(2):349–353. https://doi.org/10.1002/grl.50115
Gawarkiewicz G, Todd R, Plueddemann A, Andres M, Manning JP (2012) Direct interaction between the Gulf Stream and the shelf-break south of New England. Sci Rep 2:553. https://doi.org/10.1038/srep00553
Goddard PB, Yin J, Griffies SM, Zhang S (2015) An extreme event of sea-level rise along the Northeast coast of North America in 2009–2010. Nat Commun 6:6346. https://doi.org/10.1038/ncomms7346
Grinsted A, Moore JC, Jevrejeva S (2004) Application of the cross wavelet transform and wavelet coherence to geophysical time series. Nonlin Processes Geophys 11:561–566. https://doi.org/10.5194/npg-11-561-2004
Hughes CW, Meredith PM (2006) Coherent sea-level fluctuations along the global continental slope. Philos Trans R Soc 364:885–901. https://doi.org/10.1098/rsta.2006.1744
Huthnance JM (2004) Ocean-to-shelf signal transmission: a parameter study. J Geophys Res. https://doi.org/10.1029/2004JC002358
Kohut JT, Glenn SM, Paduan JD (2006) Inner shelf response to tropical storm Floyd. J Geophys Res Oceans. https://doi.org/10.1029/2003JC002173
Lee TN, Williams E (1988) Wind-forced transport fluctuations of the Florida current. J Phys Oceanogr 18(7):937–946. https://doi.org/10.1175/1520-0485(1988)018%3C0937:WFTFOT%3E2.0.CO;2
Levermann A, Griesel A, Hofmann M, Montoya M, Rahmstorf S (2005) Dynamic sea level changes following changes in the thermohaline circulation. Clim Dyn 24(4):347–354. https://doi.org/10.1007/s00382-004-0505-y
Little CM, Hu A, Hughes CW, McCarthy GD, Piecuch CG, Ponte RM, Thomas MD (2019) The relationship between U.S. East Coast sea level and the Atlantic meridional overturning circulation: A review. J Geophys Res Oceans 124:6435–6458. https://doi.org/10.1029/2019JC015152
Maul GA, Chew F, Bushnell M, Mayer DA (1985) Sea level variation as an indicator of Florida current volume transport: comparisons with direct measurements. Science 227(4684):304–307. https://doi.org/10.1126/science.227.4684.304
Meinen CS, Baringer MO, Garcia RF (2010) Florida current transport variability: an analysis of annual and longer-period signals. Deep-Sea Res 57(7):835–846. https://doi.org/10.1016/j.dsr.2010.04.001
Mellor GL, Hakkinen S, Ezer T, Patchen R (2002) A generalization of a sigma coordinate ocean model and an intercomparison of model vertical grids. In: Pinardi N, Woods JD (eds) Ocean Forecasting: Conceptual Basis and Applications. Springer, pp 55–72. https://doi.org/10.1007/978-3-662-22648-3_4
Montgomery RB (1938) Fluctuations in monthly sea level on Eastern US Coast as related to dynamics of Western North Atlantic ocean. J Mar Res 1(2):165–185. https://elischolar.library.yale.edu/journal_of_marine_research/527
Sweet W (2015) Accelerated sea level rise and Florida current transport. Ocean Sci 11(4):607–615. https://doi.org/10.5194/os-11-607-2015

Park K, Federico I, Di Lorenzo E, Ezer T, Cobb KM, Pinardi N, Coppini G (2022) The contribution of hurricane remote ocean forcing to storm surge along the Southeastern U.S. coast. Coast Eng 173:104098. https://doi.org/10.1016/j.coastaleng.2022.104098

Park K, Di Lorenzo E, Zhang YJ, Wang H, Ezer T, Ye F (2024) Delayed coastal inundation caused by ocean dynamics post-hurricane Matthew. Nat NPJ Clim Atmos Sci 7(5). https://doi.org/10.1038/s41612-023-00549-2

Piecuch CG, Beal LM (2023) Robust weakening of the Gulf Stream during the past four decades observed in the Florida Straits. Geophys Res Lett 50(18):2023GL105170. https://doi.org/10.1029/2023GL105170

Piecuch CG, Dangendorf S, Ponte R, Marcos M (2016) Annual sea level changes on the North American Northeast coast: influence of local winds and barotropic motions. J Clim 29:4801–4816. https://doi.org/10.1175/JCLI-D-16-0048.1

Rahmstorf S, Box J, Feulner G, Mann ME, Robinson A, Rutherford S, Schaffernicht EJ (2015) Exceptional twentieth-century slowdown in Atlantic Ocean overturning circulation. Nat Clim Chang 5:475–480. https://doi.org/10.1038/nclimate2554

Sallenger AH, Doran KS, Howd P (2012) Hotspot of accelerated sea-level rise on the Atlantic coast of North America. Nat Clim Chang 2:884–888. https://doi.org/10.1038/nclimate1597

Smeed DA, McCarthy GD, Cunningham SA, Frajka-Williams E, Rayner D, Johns WE, Meinen CS, Baringer MO, Moat B, Duchez A, Bryden HL (2014) Observed decline of the Atlantic meridional overturning circulation 2004–2012. Ocean Sci 10:29–38. https://doi.org/10.5194/os-10-29-2014

Smeed DA, Josey SA, Beaulieu C, Johns WE, Moat BI, Frajka-Williams E, Rayner D, Meinen CS, Baringer MO, Bryden HL, McCarthy GD (2018) The North Atlantic Ocean is in a state of reduced overturning. Geophys Res Lett. https://doi.org/10.1002/2017GL076350

Sturges W, Hong BG (2001) Gulf Stream transport variability at periods of decades. J Phys Oceanogr 31(5):1304–1312. https://doi.org/10.1175/1520-0485

Sweet W, Park J (2014) From the extreme to the mean: acceleration and tipping points of coastal inundation from sea level rise. Earths Future 2(12):579–600. https://doi.org/10.1002/2014EF000272

Todd RE, Asher TG, Heiderich J, Bane JM, Luettich RA (2018) Transient response of the Gulf Stream to multiple hurricanes in 2017. Geophys Res Lett 45(19):10,509-10,519. https://doi.org/10.1029/2018GL079180

Valle-Levinson A, Dutton A, Martin JB (2017) Spatial and temporal variability of sea level rise hot spots over the eastern United States. Geophys Res Lett 44:7876–7882. https://doi.org/10.1002/2017GL073926

Volkov DL, Lee S-K, Domingues R, Zhang H, Goes M (2019) Interannual sea level variability along the southeastern seaboard of the United States in relation to the gyre-scale heat divergence in the North Atlantic. Geophys Res Lett. https://doi.org/10.1029/2019GL083596

Volkov D, Zhang K, Johns W, Willis J, Hobbs W, Goes M, Zhang H, Menemenlis D (2023) Atlantic meridional overturning circulation increases flood risk along the United States southeast coast. Nat Commun 14:5095. https://doi.org/10.1038/s41467-023-40848-z

Wdowinski S, Bray R, Kirtman BP, Wu Z (2016) Increasing flooding hazard in coastal communities due to rising sea level: case study of Miami Beach, Florida. Ocean Coastal Man 126:1–8. https://doi.org/10.1016/j.ocecoaman.2016.03.002